A Novel Inhibitor of Carbonic Anhydrases Prevents Hypoxia-Induced TNBC Cell Plasticity

Annachiara Sarnella, Giuliana D'avino, Billy Samuel Hill, Vincenzo Alterio, Jean-Yves Winum, Claudiu T Supuran, Giuseppina de Simone, Antonella Zannetti

International Journal of
Molecular Sciences

MDPI

Article

A Novel Inhibitor of Carbonic Anhydrases Prevents Hypoxia-Induced TNBC Cell Plasticity

Annachiara Sarnella [1], Giuliana D'Avino [1], Billy Samuel Hill [1], Vincenzo Alterio [1], Jean-Yves Winum [2], Claudiu T. Supuran [3], Giuseppina De Simone [1] and Antonella Zannetti [1,*]

1 CNR Istituto di Biostrutture e Bioimmagini, 80122 Napoli, Italy; achiara.sarnella@gmail.com (A.S.); giul.davino@gmail.com (G.D.); bily.hill@ibb.cnr.it (B.S.H.); vincenzo.alterio@cnr.it (V.A.); gdesimon@unina.it (G.D.S.)
2 IBMM, Universite Montpellier, CNRS, ENSCM, 34296 Montpellier, France; jean-yves.winum@umontpellier.fr
3 Dipartimento NEUROFARBA, Sezione di Scienze Farmaceutiche, Università di Firenze, Sesto Fiorentino, 50139 Firenze, Italy; claudiu.supuran@unifi.it
* Correspondence: antonella.zannetti@cnr.it; Tel.: +39-3666115319

Received: 8 October 2020; Accepted: 5 November 2020; Published: 9 November 2020

Abstract: Cell plasticity is the ability that cells have to modify their phenotype, adapting to the environment. Cancer progression is under the strict control of the the tumor microenvironment that strongly determines its success by regulating the behavioral changes of tumor cells. The cross-talk between cancer and stromal cells and the interactions with the extracellular matrix, hypoxia and acidosis contribute to trigger a new tumor cell identity and to enhance tumor heterogeneity and metastatic spread. In highly aggressive triple-negative breast cancer, tumor cells show a significant capability to change their phenotype under the pressure of the hypoxic microenvironment. In this study, we investigated whether targeting the hypoxia-induced protein carbonic anhydrase IX (CA IX) could reduce triple-negative breast cancer (TNBC) cell phenotypic switching involved in processes associated with poor prognosis such as vascular mimicry (VM) and cancer stem cells (CSCs). The treatment of two TNBC cell lines (BT-549 and MDA-MB-231) with a specific CA IX siRNA or with a novel inhibitor of carbonic anhydrases (RC44) severely impaired their ability to form a vascular-like network and mammospheres and reduced their metastatic potential. In addition, the RC44 inhibitor was able to hamper the signal pathways involved in triggering VM and CSC formation. These results demonstrate that targeting hypoxia-induced cell plasticity through CA IX inhibition could be a new opportunity to selectively reduce VM and CSCs, thus improving the efficiency of existing therapies in TNBC.

Keywords: CA IX; cell plasticity; TNBC

1. Introduction

The various components of the tumor microenvironment (TME) such as stromal cells, extracellular matrix (ECM), signaling molecules, low oxygen and acidic pH control tumor cell phenotypic switching which favors the onset of chemoresistance, immune evasion, cell invasion and metastasis [1]. This ability of tumor cells to change identity through non-mutational mechanisms to cope with TME pressure is known as tumor cell plasticity and is strictly associated with the intratumoral heterogeneity of many carcinomas, causing failure of anti-cancer therapies [2]. Remarkably, the conversion of cancer cells in another lineage is generally a reversible phenomenon under the control of epigenetic and transcriptional changes [3]. Currently, there are many ongoing studies that investigate the molecular mechanisms underlying tumor cell plasticity with the aim to find new therapeutic strategies that,

targeting cellular trans-differentiation, could improve the efficiency of conventional and targeted therapies [4].

Triple-negative breast cancer (TNBC) remains the most challenging breast cancer subtype to treat not only due to the lack of ER, PgR and HER2 as therapeutic targets but also to the high heterogeneity that makes the management of this disease even more difficult [5]. Recently, through genetic profiles, TNBC was clustered into four main sub-types: Basal-like immunosuppressed (BLIS), basal-like immune activated (BLIA), mesenchymal (MES), and luminal androgen receptor (LAR) [6]. These sub-groups are characterized by distinct molecular features and show different aggressive behavior and response to therapies [7].

One of the best-known mechanisms of cell plasticity is the epithelial-to-mesenchymal transition (EMT), through which cells lose epithelial characteristics such as E-cadherin expression (a key component of epithelial cell junction), while they gain mesenchymal features including the expression of vimentin and N-cadherin [8,9]. This is a dynamic process by which tumor cells also can be in an intermediate EMT status (partial-EMT), expressing a mix of epithelial and mesenchymal markers, or they can revert to epithelial phenotype (mesenchymal-epithelial transition MET) [8,9]. The EMT program is under the control of numerous transcription factors such as SNAIL, SLUG, TWIST1/2 and ZEB1/2 that repress or induce the transcription of proteins involved in its realization. Another important example of cell plasticity is the ability of tumor cells to acquire a "cancer stem cell" (CSC)-like state comprising of a tumor cell subpopulation capability for self-renewal, tumor initiation, as well as resistance to cancer therapies [10]. Many studies have highlighted a strong relationship between EMT and CSCs because this subpopulation of tumor cells exhibits EMT markers that remain after cancer treatment, causing disease recurrence and metastasis [9]. MES-TNBC cells show a high capability to trans-differentiate in CSCs due to their intrinsic mesenchymal aggressive phenotype [10].

Importantly, MES-TNBC cells, thanks to their dynamic plasticity, can also assume an endothelial morphology and express specific markers such as VE-cadherin, thus contributing to the realization of vascular channels independent from those formed by the neo-angiogenesis process [11]. This phenomenon is known as vascular mimicry (VM) and it is associated with poor prognosis and tumor aggressiveness concerning many carcinomas including TNBC [12]. However, by not responding to antiangiogenic drugs, this functional vascular-like network can promote tumor invasion and metastasis, thus contributing to the failure of these treatments [13].

EMT program, CSC-like state and VM are closely related to each other and are under the control of the hypoxic microenvironment. Hypoxia-inducible factor-1α (HIF-1α) modulates different transcription factors such as TWIST, SNAIL, SLUG and ZEB1 and signal pathways that are reported to be involved in all three mechanisms described above [14,15]. HIF-1α also induces the expression of carbonic anhydrase IX (CA IX), a well-known cell surface pH regulating enzyme, which is an independent poor prognostic biomarker for metastases and survival in breast cancer [16]. This zinc-containing enzyme catalyzes the reversible hydration of carbon dioxide to bicarbonate and proton, thus contributing to an increase in extracellular acidosis that in turn promotes metastatic spread and drug resistance [17]. Lou et al. showed that the inhibition of CA IX caused a significant reduction of lung metastases in TNBC murine models [16]. Interestingly, it has been demonstrated that this protein is associated through its intracellular domain with the component of invadopodia matrix metalloprotease 14 (MM14) that mediates collagen degradation of ECM, favoring tumor cell invasiveness [18]. Furthermore, CA IX expression is a crucial driver of EMT and stemness markers in breast cancer and its blocking decreased CSC population in mice bearing breast cancer orthotopic xenografts [19]. Targeting CA IX with a sulfonamide inhibitor, SLC-0111, in Phase I clinical trials (NCT02215850) sensitized melanoma cells, breast cancer cells and colorectal cancer cells to chemotherapy [20] and furthermore reduced the enrichment of brain tumor-initiating cells after temozolomide treatment both in vitro and in vivo [21].

In this study, we investigated whether targeting CA IX with a novel benzoxaborole inhibitor, RC44 [22,23], which was reported to inhibit also other carbonic anhydrase isoforms including CA I, CA II and CA XII, was possible to hamper the impact of hypoxia on TNBC plasticity, thus reducing

the acquisition of stemness, invasiveness and VM capabilities through the inhibition of mesenchymal marker expression.

2. Results

2.1. CA IX Expression in TNBC Patients and in TNBC Cell Lines

Previous studies reported that CA IX expression is correlated with a more aggressive phenotype of breast cancer associated with cell invasiveness and drug resistance [16,24,25]. To investigate the potential role played by CA IX in hypoxia-induced TNBC cell plasticity, we first evaluated its expression in two public datasets: One including 55 non-triple-negative breast primary tumors and another of 198 TNBC samples. This analysis clearly showed that the expression of CA IX is higher in the TNBC group than in other breast cancers ($p < 0.0001$) (Figure 1A). Next, HIF-1α and CA IX expression levels were analyzed in two MES-TNBC cell lines, BT-549 and MDA-MB-231, grown in normoxic (21% O_2) and hypoxic (1% O_2) conditions for 48 h. As expected, TNBC cells over-expressed HIF-1α and CA IX when exposed to low O_2 levels, while in normoxia they showed no detectable HIF-1α levels, because of its oxygen-dependent degradation [26], and very low levels of CA IX. Then, CA IX expression was down-regulated by transfecting BT-549 and MDA-MB-231 cells with CA IX targeting siRNA (siRNA CA IX) for 48 h. Scrambled non-targeting siRNA (siRNA Scr) was used as a negative control. Cells transfected with siRNA Scr showed higher CA IX levels in hypoxia relative to normoxia as expected, whereas hypoxia-induced CA IX expression was strongly reduced in both cell lines treated with siRNA CA IX (Figure 1B).

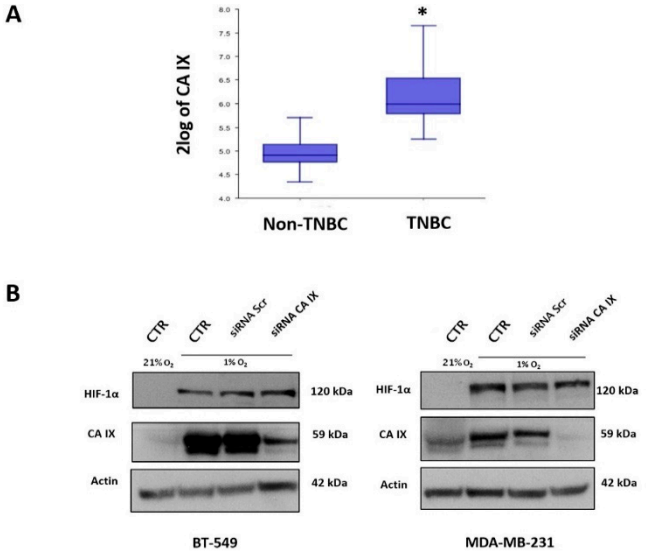

Figure 1. Analysis of carbonic anhydrase IX (CA IX) expression in triple-negative breast cancer (TNBC) sample patients and cell lines. (**A**) In silico analysis of mRNA CA IX expression was performed on two different datasets: GSE16391 which includes 55 non-triple-negative breast primary tumors and GSE76124 which includes 198 TNBC tumors from MD Anderson Cancer Center. The box plot represents a comparison of the CA IX expression between non-TNBC and TNBC tumor samples * $p < 0.0001$. (**B**) MDA-MB-231 and BT-549 cells were transfected for 48 h with CA IX-specific siRNAs (100 nM) or non-targeting siRNAs (siRNA Scr) (100 nM), used as negative control, in 1% O_2. A control was performed in 21% O_2. CA IX protein levels were analyzed using Western blot analysis. Actin was used as loading control. Representative data from one of three experiments are shown.

2.2. Inhibition of CA IX Prevents Vasculogenic Mimicry in TNBC Cells

In order to investigate the ability of TNBC cells to switch in an endothelial-like phenotype and organize themselves into vascular-like structures, we seeded BT-549 and MDA-MB-231 cells on the

surface of Matrigel to establish the 3D culture model for assessing VM development during 24 h. As shown in Figure 2, the ability to form channel-like structures of BT-549 and MDA-MB-231 cells was increased two-fold when they were grown under hypoxic conditions in comparison to normoxia. The down-regulation of CA IX expression by siRNA CA IX drastically reduced hypoxia-dependent enhancement of vessel loop formation in both cell lines (reduction of 71.15%, $p < 0.0001$ in BT-549 cells; reduction of 74.60%, $p < 0.0001$ in MDA-MB-231 cells), whereas cell transfection with siRNA Scr did not cause any change. Interestingly, when TNBC cells were treated with a novel CA inhibitor, RC44 (100 µM) (RC44 chemical structure is shown in (Figure 3A), for 24 h, a very strong inhibition of VM was observed in comparison with untreated cells (reduction of 78.85% and $p < 0.0001$ in BT-549 cells; reduction of 90.48% and $p < 0.0001$ in MDA-MB-231 cells) (Figure 2). RC44 did not cause any reduction of VM with respect to the control when experiments were carried out under normoxic conditions (Figure S1). Furthermore, the effect of RC44 on cell viability was tested and any significant change was observed at 100 µM after 72 h of treatment (Figure 3B). In addition, acidification of the extracellular medium in hypoxia was inhibited by RC44 100 µM in both TNBC cell lines (Figure 3C).

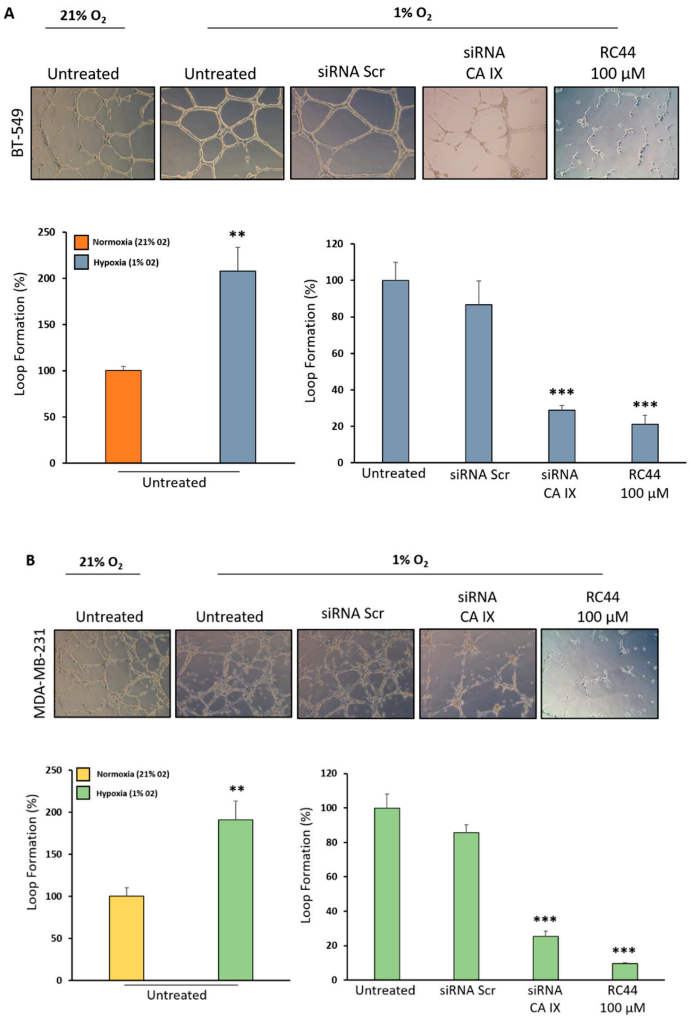

Figure 2. Targeting CA IX reduces TNBC vasculogenic mimicry. BT-549 (**A**) and MDA-MB-231 (**B**) were grown in normoxia (21% O_2) or hypoxia (1% O_2) conditions on the surface of Matrigel and vascular loops were analyzed. TNBC cell grown in 1% O_2 were transfected with siRNA CA IX (100 nM) and siRNA Scr (100 nM) for 48 h or treated with RC44 (100 µM) and seeded into 24-well plates pre-coated with 80 µL/well Matrigel. Representative images were taken at 10× and the average of the number of complete loops was calculated from 3–5 random fields by a macro made with ImageJ software. Bars depict mean ± SD of three independent experiments. *** $p < 0.0001$; ** $p < 0.001$.

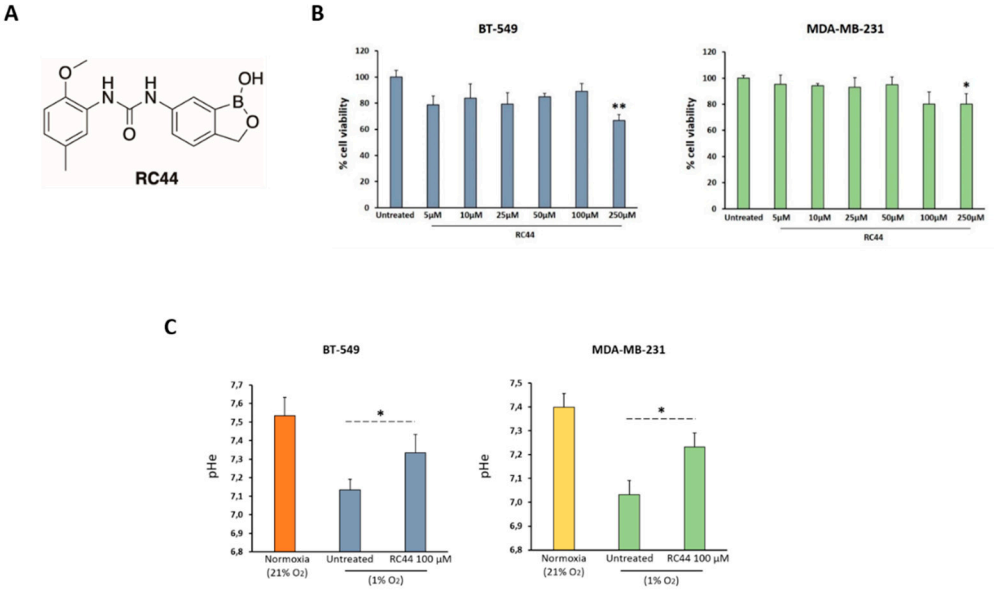

Figure 3. (**A**) Chemical Structure of CA inhibitor RC44. (**B**) Effect of CA inhibitor RC44 on TNBC cell proliferation. Cell viability (MTS assay) of BT-549 and MDA-MB-231 (50×10^3 cells/well), treated with different concentrations of RC44 (from 5 μM to 250 μM) for 72 h in hypoxic conditions (1% O_2). All the data are expressed as percentage of viable cells, considering the untreated control cells as 100%. (**C**) Effect of RC44 on extracellular pH (pHe) in hypoxia. BT-549 and MDA-MB-231 were grown under normoxic (21% O_2) and hypoxic conditions (1% O_2) for 72 h and treated with RC44 (100 μM) when grown in hypoxia. Bars depict mean ± SD of three independent experiments. (** $p < 0.001$; * $p < 0.01$).

2.3. Targeting CA IX Reduces Hypoxia-Induced Migration and Invasion of TNBC Cells

Having established the role of CA IX in promoting VM and the effect of RC44 to hamper this phenomenon associated with more aggressive behavior of TNBC, next we investigated whether RC44 could interfere with TNBC cell ability to migrate and invade the extracellular matrix. To this end, we performed trans-well migration and invasion assays using 10% FBS as chemo-attractant (1% FBS was used as negative control) under normoxic and hypoxic conditions. We observed a three-fold increase in cell chemotactic capability when TNBC cell lines were grown in the presence of 1% O_2 in comparison with 21% O_2 (Figure 4). The cell transfection with siRNA CA IX caused a significant delay in BT-549 and MDA-MB-231 cell migration (87.83% and 75.18% reduction, respectively, $p < 0.0001$) with respect to control and siRNA Scr under hypoxic conditions (Figure 4). Notably, a strong inhibition of cell migration was also observed in both cell lines treated with 100 μM RC44 with respect to untreated and siRNA Scr treated cells (reduction of 90.82%, $p < 0.0001$ in BT-549 cells; reduction of 60.03%, $p < 0.0001$ in MDA-MB-231 cells) (Figure 4).

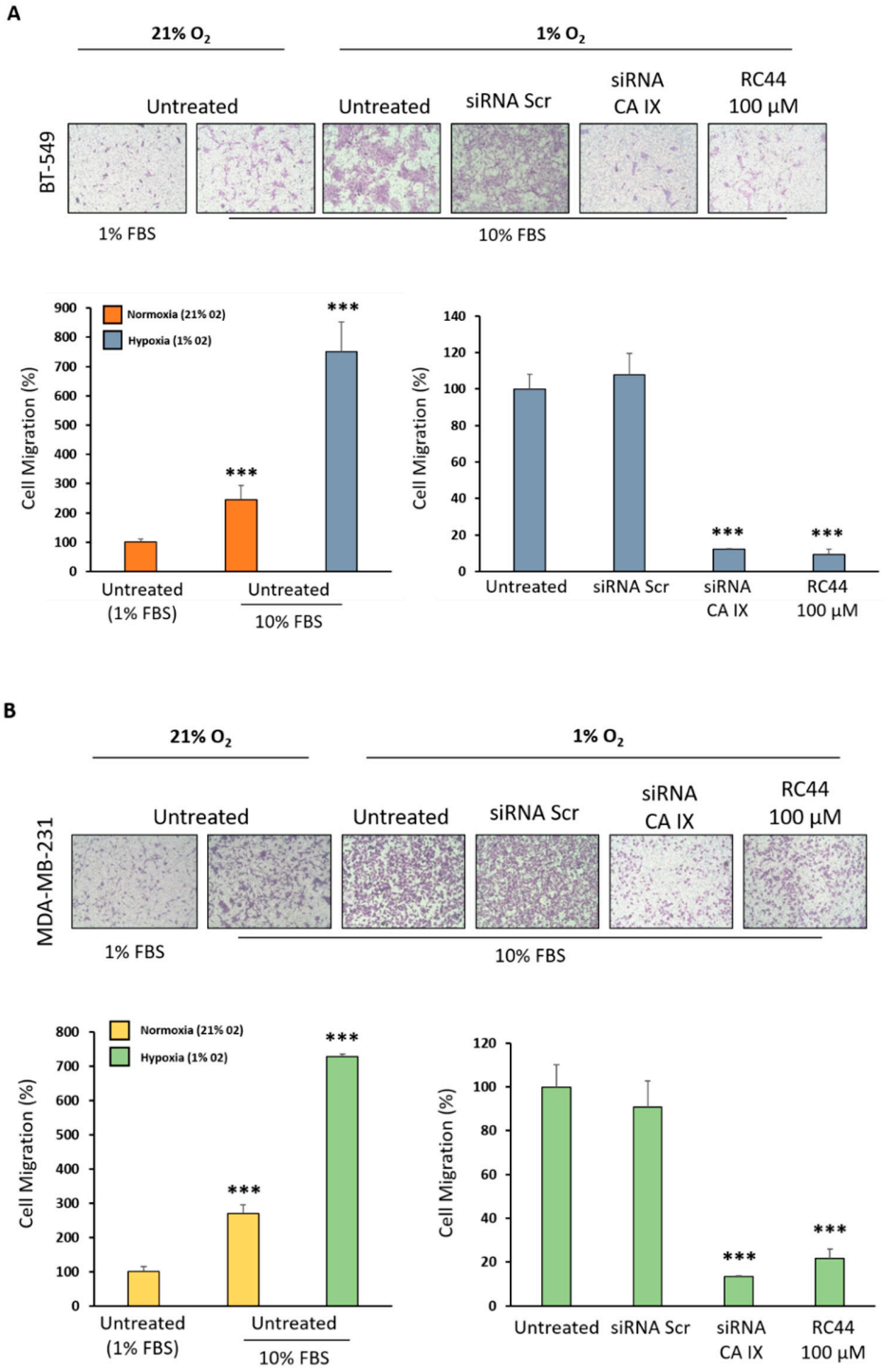

Figure 4. Targeting CA IX hampers TNBC cell migration. Boyden chamber was used for migration assay. BT-549 (**A**) and MDA-MB-231 (**B**) were grown in normoxia (21% O_2) or hypoxia (1% O_2) conditions and migration was analyzed. Medium containing 1% FBS or 10% FBS was added to the lower chamber as chemoattractant. The results are expressed as the percentage of migrating cells considering the untreated control sample (1% FBS) as 100%. TNBC cells grown in 1% O_2 were transfected with siRNA CA IX (100 nM) and siRNA Scr (100 nM) or treated with RC44 (100 µM) and seeded in the upper chamber. Medium containing 10% FBS was added to the lower chamber as chemoattractant. The results are expressed as the percentage of migrating cells considering the untreated control sample (10% FBS) as 100%. Bars depict mean ± SD of three independent experiments. *** $p < 0.0001$.

Furthermore, the effect of RC44 in hampering TNBC cell migration mediated by hypoxia was also assessed by wound healing assay. Monolayers of MDA-MB-231 and BT-549 cells were scratched and images were taken at 0 and 24 h after wounding. We observed that CA inhibitor caused a significant decrease of wound healing in both TNBC cell lines (BT-549 cells: 56.15%, $p < 0.0001$; MDA-MB-231 cells: 65.02%, $p < 0.0001$) in comparison with control (Figure 5).

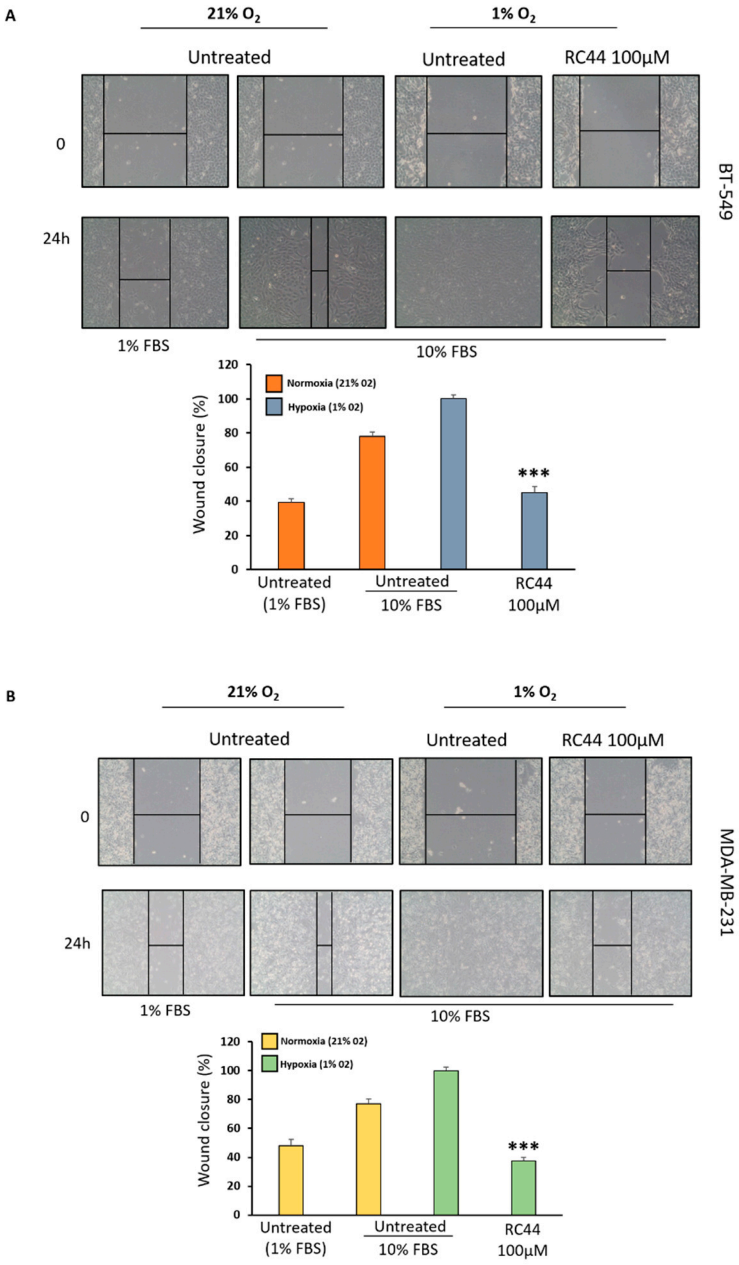

Figure 5. Effect of CA inhibitor RC44 on cell wound healing ability. BT-549 (**A**) and MDA-MB-231 (**B**) were grown in normoxia (21%O_2) or hypoxia (1%O_2) conditions and were scratched with pipette tips to create wounds. After removal of detached cells, medium containing 1% FBS, 10% FBS and RC44 (100 µM) were added to cells. Each scratch area was photographed at 0, 24 h. The distance between the edges of the scratch was measured by ImageJ, the average distance was quantified and the extent of wound closure was determined as follows: Wound closure (%) = 1 − (wound width tx/wound width t0) × 100. Bars depict mean ±SD of three independent experiments. *** $p < 0.0001$.

The ability of RC44 to block TNBC cell invasiveness due to the hypoxic microenvironment was analyzed using a trans-well coated with Matrigel mimicking the extracellular matrix. As expected, the

cells grown in low oxygen (1%) showed higher invasiveness than those grown in normoxia (21% O_2), whereas when they were transfected with siRNA CA IX a dramatic reduction of their ability to invade Matrigel was observed (68.54%, $p < 0.0001$ in BT-549 cells; 82.78%, $p < 0.0001$ in MDA-MB-231 cells) (Figure 6). Similarly, the addition of RC44 (100 µM) for 72 h caused a significant inhibition of TNBC cell invasiveness ($p < 0.0001$) thus preventing TNBC pre-metastatic phenotype (Figure 6).

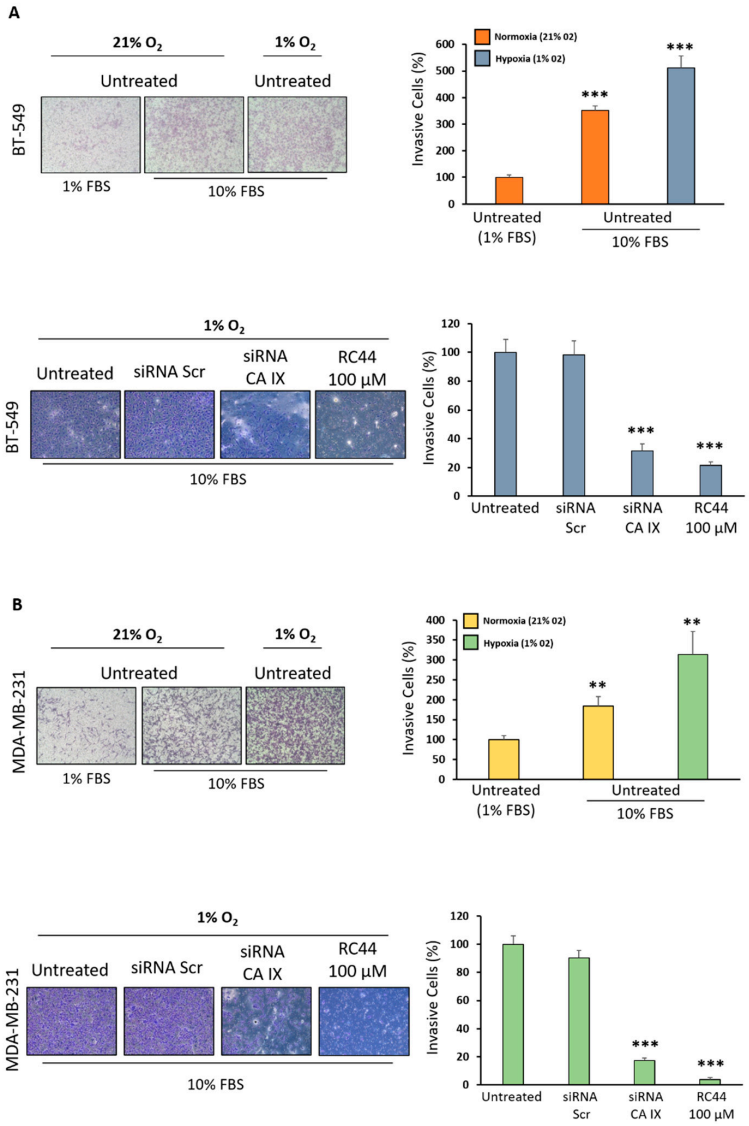

Figure 6. Blocking CA IX inhibits TNBC invasiveness. Boyden chamber coated with Matrigel to mimic ECM was used for cell invasion assay. BT-549 (**A**) and MDA-MB-231 (**B**) were grown in normoxia (21% O_2) or hypoxia (1% O_2) conditions and their invasion ability was analyzed. Medium containing 1% FBS or 10% FBS was added to the lower chamber as chemoattractant. The results are expressed as the percentage of invasive cells considering the untreated control sample (1% FBS) as 100%. TNBC cells grown in 1% O_2 were transfected with siRNA CA IX (100 nM) and siRNA Scr (100 nM) or treated with RC44 (100 µM) and seeded in the upper chamber. Medium containing 10% FBS was added to the lower chamber as chemoattractant. The results are expressed as the percentage of invasive cells considering the untreated control sample (10% FBS) as 100%. Bars depict mean ±SD of three independent experiments. *** $p < 0.0001$; ** $p < 0.001$.

2.4. Targeting CA IX Inhibits TNBC Mammosphere Formation

Recently, Sun et al. (2019) showed that cancer stem-like cells directly participate in VM in TNBC [13]. Therefore, to elucidate the involvement of CA IX in CSC formation, BT-549 and MDA-MB-231 cells were grown under anchorage-independent serum-free culture conditions to form mammospheres with stemness features as shown by overexpression of nanog and sox-2 (Figure S2). Both TNBC cell lines grown in a hypoxic microenvironment showed a significant enhancement of number and size of spheroids with respect to cells grown in normoxia. BT-549 cells were capable of forming spheroids more efficiently than MDA-MB-231 cells. The down-regulation of CA IX expression by specific siRNA as well as the treatment with RC44 of TNBC cells reduced TNBC cell ability to form non-adherent mammospheres with stemness characteristics in hypoxic TME (Figure 7). RC44 did not cause any change in spheroid number and size with respect to the control when experiments were carried out under normoxic conditions (Figure S3).

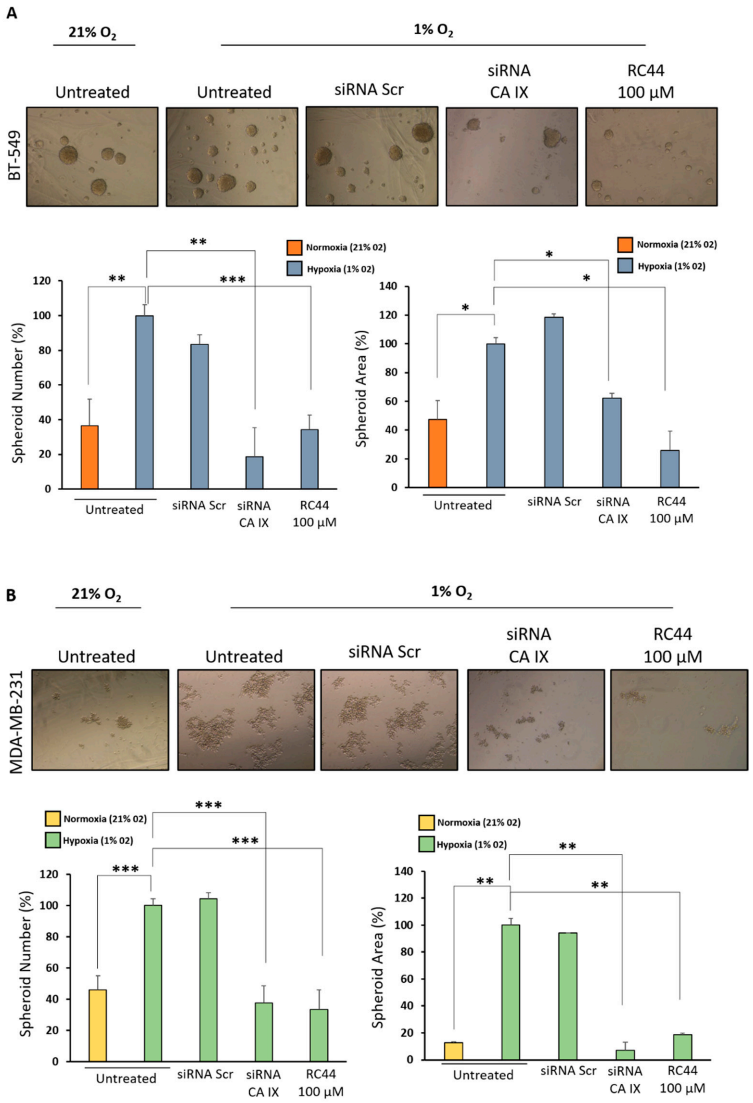

Figure 7. Targeting CA IX reduces the transformation of TNBC cells in cancer stem-like cells. BT-549 (**A**) and MDA-MB-231 (**B**) cells were seeded in ultra-low attachment multiwall plates and grown in serum-free DMEM supplemented with B27,

bFGF (20 ng/mL) and EGF (10 ng/mL) in normoxic and hypoxic conditions for seven days. TNBC cells grown in 1% O_2 were transfected with siRNA CA IX (100 nM) and siRNA Scr (100 nM) or treated with RC44 (100 μM) and grown as described above. Spheroid formation was analyzed under a phase-contrast microscopy and size and number of formed spheroids was calculated using ImageJ. Bars depict mean ± SD of three independent experiments. *** $p < 0.0001$; ** $p < 0.001$; * $p < 0.01$.

2.5. Targeting CA IX Reduces Markers Associated with Stemness and Vasculogenic Mimicry

Finally, on the basis of the link between these various forms of cell plasticity induced by hypoxia through CA IX up-regulation, we shed light on the commune underlying signal pathways. We found that RC44 down-regulated β-catenin expression, a protein well known to be correlated with stemness and EMT, which has been reported to reduce cell adhesion interacting with CA IX [27]. Furthermore, CA IX inhibition caused a reduction of expression levels of both transcriptional factors Zeb-1 and Slug involved in the occurrence of all mechanisms described above through the regulation of mesenchymal marker expression [28,29]. In addition, the cell treatment with RC44 provoked a dramatic reduction of mesenchymal markers N-cadherin and vimentin expression levels, which are associated with aggressive phenotype of the MES-TNBC sub-group. In agreement with other studies, the effect of RC44 on N-cadherin expression was observed only in BT-549 cells because this protein is not expressed in MDA-MB-231 cells (Figure 8A). Similar results were obtained when CA IX expression was down-regulated by specific siRNA (Figure 8B).

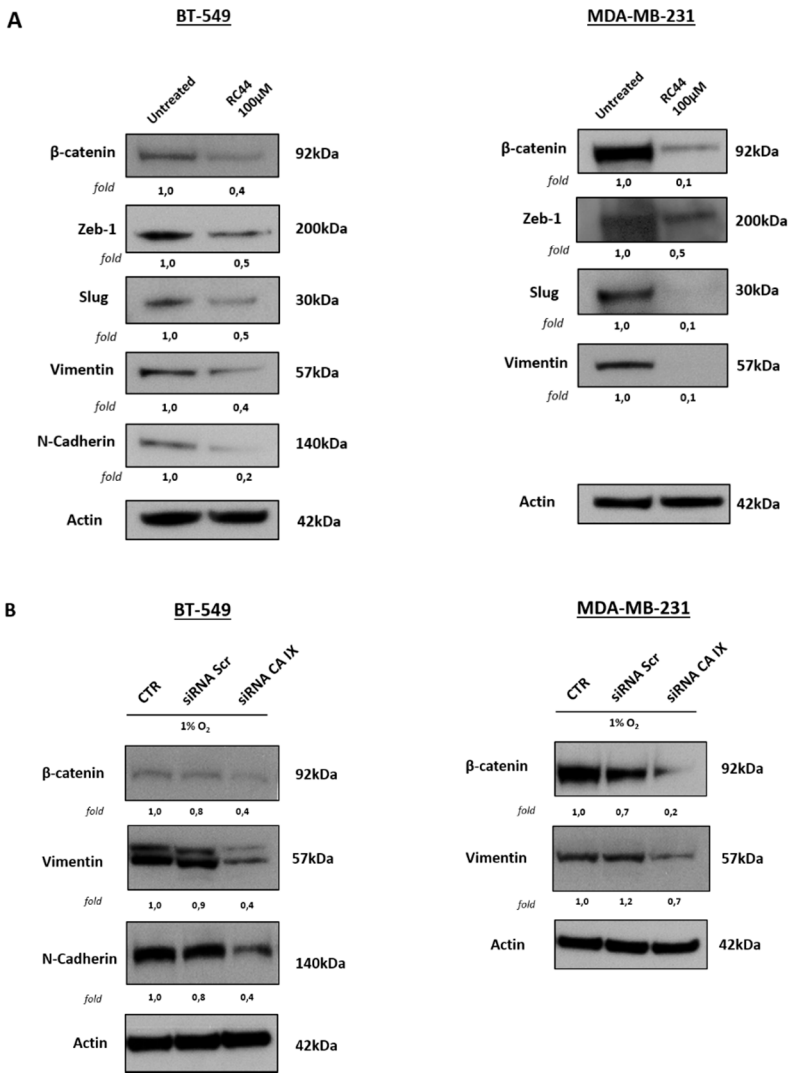

Figure 8. RC44 and CA IX-specific siRNAs reduces signal pathways associated with TNBC plasticity. (**A**) Analysis by Western blot of Vimentin, N-cadherin, β-catenin, Zeb-1 and Slug levels in untreated and RC44 treated BT-549 and MDA-MB-231 cells. (**B**) TNBC cells were transfected for 48 h in hypoxia (1% O_2) with CA IX-specific siRNAs (100 nM) or non-targeting siRNAs (siRNA Scr) (100 nM) used as negative control. Vimentin, N-cadherin and β-catenin level protein levels were analyzed using Western blot analysis. Actin was used as loading control. Representative data from one of three experiments are shown.

3. Discussion

TNBC remains the most challenging breast cancer subtype to treat not only for the lack of ER, PgR and HER2 as therapeutic targets but also for the high heterogeneity that makes the management of this disease even more difficult [30]. While there are numerous efforts to classify TNBC into distinct clinical and molecular subtypes and find specific biomarkers to guide treatment decisions [31], currently chemotherapy remains the standard of care for TNBC patients. Unfortunately, this disease is characterized by a highly aggressive clinical course, worse prognosis and many patients that initially respond to conventional therapies subsequently develop drug resistance, relapse and metastases [5]. These malignant features are linked to the high pliability of tumor cells to adapt to unfavorable TME, allowing them to survive and invade other tissues [3]. In our previous studies we demonstrated the ability of mesenchymal TNBC cells to modify their identity and acquire a new more aggressive phenotype through αvβ3 and/or EGFR [32,33]. Here, we investigated the crucial role played by

the hypoxic conditions of TME in favoring and increasing the lineage plasticity of TNBC cells, thus promoting tumor cell diversity and driving intratumoral heterogeneity. Hypoxic TME arises because of the oxygen deficit due to a highly abnormal vasculature; TNBC cells can overcome this disadvantage, transdifferentiating into endothelial cells for forming vessel-like structures [34]. It has been observed in many types of carcinomas that VM is associated with high expression of hypoxia-inducible factor-1α (HIF-1α) and correlated with EMT program [35,36].

Numerous pieces of evidence have demonstrated the crucial role played by CA IX, an enzyme involved in pH regulation and transcriptionally regulated by HIF-1α in malignant progression of solid tumors [17,37]. Interestingly, CA IX does not express in normal tissues except for gastric epithelium, where it plays a protective role from acid load [37]. CA IX supports tumor cells to adapt themselves to hypoxia and intracellular acidification, thus contributing to increasing their ability to migrate, to invade ECM and to resist conventional treatments [17,37]. Remarkably, CA IX expression was found to be associated with metalloproteinases/invadopodia-mediated invasion and stemness in TNBC cells [18,19]. In this study, for the first time, we demonstrate the involvement of CA IX in hypoxia-induced VM in TNBC. Targeting this protein with a specific siRNA drastically reduced vessel-like structure formation. Similar results were obtained using RC44, a novel CA benzoxaborole inhibitor, which hampered the ability of TNBC cells to assume an endothelial phenotype. Furthermore, RC44 caused a strong inhibition of cell migration and invasiveness, reducing the metastatic potential of TNBC. These results are in agreement with those recently reported by Ciccone et al. that show how the pharmacological inhibition of CA IX induces tumor cell death by activating the apoptotic pathway involving p53 and caspase-3, and reduces cell invasion, inducing the switch from the mesenchymal phenotype toward an epithelial one [38]. Recently, Guerrini et al. reported the involvement of CA XII in TNBC progression through its crosstalk with hedgehog pathway [39]; therefore, given that RC44 is able to inhibit also this isoform, we believe that this molecule may be more helpful in the treatment of this aggressive carcinoma.

It is well established that there is a close connection between VM, stemness and EMT program regulated by hypoxia [34–36,40–42]. Interestingly, Sun et al. showed that cancer stem-like cells directly participate in VM in TNBC [13]. Furthermore, CSCs play a crucial role in drug resistance because, being able to survive to conventional treatments, they can cause metastases and disease relapse. Interestingly, it has been demonstrated that CA IX inhibition causes depletion of CSCs in a breast cancer animal model [19]. Therefore, here we investigated whether inhibiting CA IX with RC44 could impair the increase of hypoxia-induced TNBC cell transformation in CSCs. The cell treatment with this molecule reduced the ability to form non-adherent mammospheres with stemness characteristics in hypoxic TME. Finally, on the basis of the link between these various forms of cell plasticity induced by hypoxia through CA IX up-regulation, we shed light on the commune underlying signal pathways. We found that RC44 down-regulated β-catenin expression, a protein well known to be correlated with stemness and EMT, which has been reported to reduce cell adhesion interacting with CA IX [27]. CA IX inhibition also caused a reduction of levels of both transcriptional factors ZEB1 and Slug involved in the occurrence of all mechanisms described above through the regulation of mesenchymal marker expression [28,29]. In addition, cell treatment with RC44 provoked a dramatic reduction of N-cadherin and vimentin expression, which is associated with the aggressive phenotype of the MES-TNBC sub-group.

4. Materials and Methods

4.1. In Silico Analysis of the Expression of CA IX in TNBC

For CA IX mRNA expression analysis and correlation with clinical, molecular and cell phenotype, the Genomics Analysis and Visualization platform (R2: Genomics analysis and visualization platform; http://r2.amc.nl) was used. The analysis was performed with the following datasets: GSE16391, which includes 55 non-triple-negative breast primary tumors and GSE76124, which includes 198 TNBC tumors

from the MD Anderson Cancer Center (Houston, Texas, USA) [43]. The correlation was assessed by one-way analysis of variance (ANOVA), through the R2 platform and presented in box plots.

4.2. Cell Lines and Culture Conditions

The triple-negative breast cancer cell lines came from the American Type Culture Collection (ATCC, Manassas, VA) and were cultured in the Roswell Park Memorial Institute (RPMI) 1640 Medium supplemented with 10% fetal bovine serum (FBS) and 1% L-glutamine-penicillin-streptomycin and grown at 37 °C with 5% CO_2. All experiments were performed by growing MDA-MB-231 and BT-549 in normoxic (21% O_2) and hypoxic conditions (1% O_2). Hypoxia was attained in a modular incubator chamber (Stem Cell, Catalog #27310). The chamber was flooded with the hypoxic gas mixture for 7 min and then sealed and stored in an incubator at 37 °C in 5% CO_2. The normoxic control was stored in the same incubator for the same amount of time [43,44].

4.3. Cell Viability Assay

The viability of MDA-MB-231 and BT-549 cells (5.0 x 10^3 cells/well, 96-well plates), untreated and treated with RC44 at different concentrations, was assessed with CellTiter 96 AQueous One Solution Cell Proliferation Assay (Promega BioSciences Inc., Fitchburg, WI, USA) using 3-(4,5-dimethylthiazol-2yl)-5-(3-carboxymethoxy-phenyl)-2-(4-sulfophenyl)-2H tetrazolium (MTS), and according to the manufacturer's instructions.

4.4. RNA Interference

CA IX-targeting siRNA (L-005244-00) and a corresponding control non-targeting siRNA (D-001810-10-05) were purchased from Dharmacon. MDA-MB-231 and BT-549 were transfected for 48 h using Dharmacon siRNA transfection reagent and 100 nmol/L siRNAs according to the manufacturer's protocol. MDA-MB-231 and BT-549 cells were grown in a culture medium after transfection in hypoxic conditions (1% O_2) and the down-regulation of targeted protein expression was assessed using Western blot analysis [45].

4.5. RC44 Synthesis

RC44 was prepared according to our previous study [22].

4.6. Measurement of Extracellular pH

Analysis of extracellular pH changes was performed as previously described by Lou, Y. et al. [16].

Briefly, cells were grown under normoxic (21% O_2) and hypoxic conditions (1% O_2) in subconfluent status for 72 h and treated with RC44 100 µM when grown in the presence of 1% O_2. Media were collected and pH was measured immediately using a digital pH meter.

4.7. Vascular Mimicry

Harvested MDA-MB-231 (1×10^4 cells) and BT-549 (8×10^5 cells) were suspended in a 100 µl medium containing 2% FBS in the presence or absence of RC44 (100 µM), siRNA Scr (100 nM) and siRNA CA IX (100 nM). Treated cells were then seeded into 24-well plates pre-coated with 80 µL/well Matrigel and incubated at 37 °C and 5% CO_2 for 24 h. Tube formation was analyzed under a phase-contrast microscopy and complete loops were quantified by a macro made with the ImageJ software [32].

4.8. Spheroid Formation Assay of TNBC Cells

BT-549 and MDA-MB-231 cells (5×10^4/well) were seeded in ultra-low attachment 6-multiwell-plates (Corning) and grown in serum-free DMEM supplemented with B27 (1×), bFGF (20 ng/mL) EGF (10 ng/mL). Cells were incubated at 37 °C with 5% CO_2 for 7 days. Spheroid formation

was analyzed under a phase-contrast microscopy and the size and number of formed spheroids were calculated using ImageJ [33].

4.9. Cell Migration Assay

Cell migration was performed as previously reported using 24-well Boyden chambers (Corning, NY) with inserts of polycarbonate membranes (8 μm pores). MDA-MB-231 and BT-549 cells (0.5×10^5/well) were re-suspended in 100 μL of serum-free medium in the presence or absence of RC44 (100 μM), siRNA Scr (100 nM) and siRNA CA IX (100 nM) (Dharmacon, CO, USA) and seeded in the upper chamber [46,47]. After the addition of 1% FBS or 10% FBS in the lower chamber as chemo-attractants, the trans-wells were put in a humidified incubator in 5% CO_2 for 24 h at 37 °C. The non-migrated cells were removed with cotton swabs, whereas the cells that had migrated were visualized by staining the membrane with 0.1% crystal violet in 25% methanol. 10 random fields/filter were counted under a phase contrast microscope (Leica) and images were captured using a digital camera (Canon). All experiments were performed at least three times. All the results are expressed as the percentage of migrating cells considering the untreated control sample as 100%.

4.10. Wound Healing Assay

An in vitro wound model was performed using a scratch assay. MDA-MB-231 and BT-549 cells grown as confluent monolayers in 6-well plates were scratched with pipette tips to create wounds. After the removal of detached cells, mediums containing 1% FBS, 10% FBS and RC44 (100 μM) were added to cells and the plates were incubated at 37 °C in a humidified incubator in 5% CO_2 for 24 h. Each scratch area was photographed at 0 and 24 h. The distance between the edges of the scratch was measured by ImageJ, the average distance was quantified and the extent of wound closure was determined as follows: Wound closure (%) = 1 − (wound width tx/wound width t0) × 100 [48]. All experiments were performed at least three times.

4.11. Cell Invasion Assay

The invasion assay was performed using the Boyden chamber with membranes (8 μm pores) coated with 50 μL of diluted Matrigel (1:5 in PBS) (Corning, NY, USA). MDA-MB-231 and BT-549 cells (1×10^5/100 μL serum-free medium per well) were harvested, suspended in serum free medium alone or containing RC44 (100 μM), siRNA Scr (100 nM) and siRNA CA IX (100 nM) and placed in the top chamber. In the lower chamber, a medium containing 1% FBS or 10% FBS was added and used as chemo-attractant. Cells were allowed 72 h to invade in a humidified incubator with 5% CO_2 at 37 °C. To visualize and analyze invading cells, the same experimental procedure described above for cell migration assay was performed. All experiments were performed at least three times.

4.12. Cell Lysate Preparation and Western Blot Analysis

Whole-cell lysates and Western blot analysis were performed as previously described. An equal amount of proteins from cells were separated by 4–12% SDS-PAGE and were transferred to a nitrocellulose membrane. Blots were blocked for 1 h with 5% non-fat dry milk and then incubated over night with the following primary antibodies: Anti-HIF-1α (BD Biosciences), anti-Zeb-1, anti-N-cadherin, anti-β-catenin, anti-Vimentin, anti-Slug (CST-9782; Cell Signaling Technology Inc), anti-CA IX (R&D), anti-Sox-2, anti-Nanog (CST-9093; Cell Signaling Technology Inc., Beverly, MA, USA), anti-Actin (A4700; Sigma-Aldrich, Saint Luis, MO, USA) and anti-Vinculin (Santa Cruz Biotechnology, Inc., Heidelberg, Germany). After washing with 0.1% Tween-20 in PBS, the filters were incubated with their respective secondary antibodies for 1 h and analyzed using the ECL system. Densitometric analyses were performed on at least two different expositions to assure the linearity of each acquisition using ImageJ software (v1.46r) [49,50].

4.13. Statistical Analysis

Results were obtained from at least three independent experiments and are expressed as means ± standard deviation. Data were analyzed with GraphPad Prism statistical software 6.0 (GraphPad Software, La Jolla, CA, USA) and significance was determined using Student's t test. A p value < 0.05 was considered statistically significant.

5. Conclusions

In conclusion, our results indicate that CA IX may be a suitable and specific biomarker for monitoring TNBC aggressiveness due to its involvement in helping cancer cells to adapt to the hostile hypoxic and acidic microenvironment through cell phenotype switching. Furthermore, the inhibition of this enzyme by a novel therapeutic agent RC44, preventing the emergence of hypoxia-induced cell plasticity, could be a novel strategy for improving the efficiency of conventional and targeted therapies (Figure 9). Further studies are planned to validate the efficacy of the molecule in vivo.

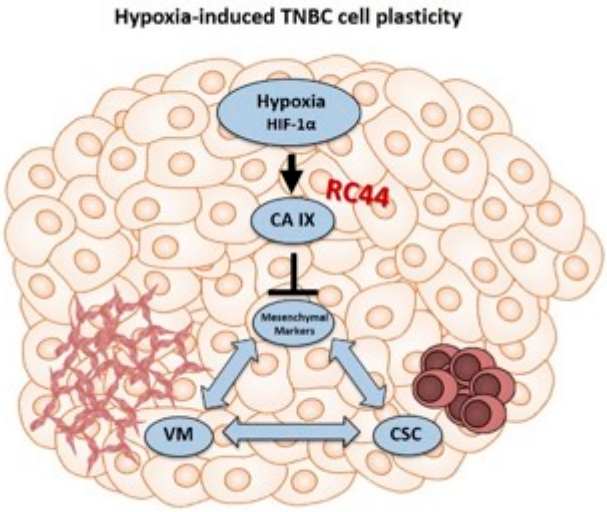

Figure 9. Schematic model illustrating that targeting hypoxia-induced cell plasticity through CA IX inhibition could be a new opportunity to selectively hamper VM and CSCs through mesenchymal marker inhibition. (Hypoxia-inducible factor (HIF-1α); carbonic anhydrase IX (CA IX); vascular mimicry (VM); cancer stem cell (CSC).).

Supplementary Materials: The following are available online at http://www.mdpi.com/1422-0067/21/21/8405/s1.

Author Contributions: Concept and design: A.Z., G.D.S., J.-Y.W., C.T.S.; experiments performed by: A.S., G.D., B.S.H., V.A.; materials and other analytical tools: A.Z., J.Y.W., G.D.S., V.A.; writing the manuscript: A.Z.; writing-review and editing: A.Z., G.D.S., J.-Y.W., C.T.S., V.A. All authors have read and agreed to the published version of the manuscript.

Funding: This work was supported by grants from MIUR-PON "Ricerca e Innovazione" 2014-2020 (grant MOLIM ONCOBRAIN LAB), from Regione Campania PO FESR 2014-2020 (grant eMORFORAD) and partially funded from MIUR Progetti di Ricerca di Rilevante Interesse Nazionale (PRIN) Bando 2017-grant 2017MHJJ55. A.S. fellowship was supported by grant from MIUR Progetti di Ricerca di Rilevante Interesse Nazionale (PRIN) Bando 2017-grant 2017MHJJ55.

Acknowledgments: DiSTABiF and Università della Campania Luigi Vanvitelli coordinating program followed by A.S.

Conflicts of Interest: The authors declare no conflict of interest.

References

1. Hill, B.S.; Sarnella, A.; D'Avino, G.; Zannetti, A. Recruitment of stromal cells into tumour microenvironment promote the metastatic spread of breast cancer. *Semin. Cancer. Biol.* **2020**, *60*, 202–213.
2. Yuan, S.; Norgard, R.J.; Stanger, B.Z. Cellular plasticity in cancer. *Cancer Discov.* **2019**, *9*, 837–851.
3. Quintanal-Villalonga, A.; Chan, J.M.; Yu, H.A.; Pe'er, D.; Sawyers, C.L.; Triparna, S.; Charles, M.R. Lineage plasticity in cancer: A shared pathway of therapeutic resistance. *Nat. Rev. Clin. Oncol.* **2020**, *17*, 360–371.
4. Boumahdi, S.; De Sauvage, F.J. The great escape: Tumour cell plasticity in resistance to targeted therapy. *Nat. Rev. Drug Discov.* **2020**, *19*, 39–56.
5. Bianchini, G.; Balko, J.M.; Mayer, I.A.; Sanders, M.E.; Gianni, L. Triple-negative breast cancer: Challenges and opportunities of a heterogeneous disease. *Nat. Rev.* **2016**, *13*, 674–690.
6. Burstein, M.D.; Tsimelzon, A.; Poage, G.M.; Covington, K.R.; Contreras, A.; Fuqua, S.A.; Savage, M.I.; Osborne, C.K.; Hilsenbeck, S.G.; Chang, J.C.; et al. Comprehensive genomic analysis identifies novel subtypes and targets of triple-negative breast cancer. *Clin. Cancer Res.* **2015**, *21*, 1688–1698.
7. Lehmann, B.D.; Bauer, J.A.; Chen, X.; Sanders, M.E.; Chakravarthy, A.B.; Shyr, Y.; Pietenpol, J.A. Identification of human triple-negative breast cancer subtypes and preclinical models for selection of targeted therapies. *J. Clin. Investig* **2011**, *121*, 2750–2767.
8. Lamouille, S.; Xu, J.; Derynck, R. Molecular mechanisms of epithelial-mesenchymal transition. *Nat. Rev. Mol. Cell Biol.* **2014**, *15*, 178–196.
9. Shibue, T.; Weinberg, R.A. EMT, CSCs, and drug resistance: The mechanistic link and clinical implications. *Nat. Rev. Clin. Oncol.* **2017**, *14*, 611–629.
10. O'Conor, C.J.; Chen, T.; González, I.; Cao, D.; Peng, Y. Cancer stem cells in triple-negative breast cancer: A potential target and prognostic marker. *Biomark. Med.* **2018**, *12*, 813–820.
11. Liu, T.J.; Sun, B.C.; Zhao, X.L.; Zhao, X.M.; Sun, T.; Gu, Q.; Yao, Z.; Dong, X.Y.; Zhao, N.; Liu, N. CD133+ cells with cancer stem cell characteristics associates with vasculogenic mimicry in triple-negative breast cancer. *Oncogene* **2013**, *32*, 544–553.
12. Andonegui-Elguera, M.A.; Alfaro-Mora, Y.; Cáceres-Gutiérrez, R.; Caro-Sánchez, C.H.S.; Herrera, L.A.; Díaz-Chá, J. An overview of vasculogenic mimicry in breast cancer. *Front. Oncol.* **2020**, *10*, 220.
13. Sun, H.; Yao, N.; Cheng, S.; Li, L.; Liu, S.; Yang, Z.; Shang, G.; Zhang, D.; Yao, Z. Cancer stem-like cells directly participate in vasculogenic mimicry channels in triple-negative breast cancer. *Cancer Biol. Med.* **2019**, *16*, 299–311.
14. Tam, S.Y.; Wu, V.W.C.; Law, H.K.W. Hypoxia-induced epithelial-mesenchymal transition in cancers: HIF-1α and beyond. *Front. Oncol.* **2020**, *10*, 486.
15. Xiang, L.; Semenza, G.L. Hypoxia-inducible factors promote breast cancer stem cell specification and maintenance in response to hypoxia or cytotoxic chemotherapy. *Adv. Cancer Res.* **2019**, *141*, 175–212.
16. Lou, Y.; McDonald, P.C.; Oloumi, A.; Chia, S.; Ostlund, C.; Ahmadi, A.; Kyle, A.; Auf dem Keller, U.; Leung, S.; Huntsman, D.; et al. Targeting tumor hypoxia: Suppression of breast tumor growth and metastasis by novel carbonic anhydrase IX inhibitors. *Cancer Res.* **2011**, *71*, 3364–3376.
17. Supuran, C.T.; Alterio, V.; Di Fiore, A.; D'Ambrosio, K.; Carta, F.; Monti, S.M.; De Simone, G. Inhibition of carbonic anhydrase IX targets primary tumors, metastases, and cancer stem cells: Three for the price of one. *Med. Res. Rev.* **2018**, *38*, 1799–1836.
18. Swayampakula, M.; McDonald, P.C.; Vallejo, M.; Coyaud, E.; Chafe, S.C.; Westerback, A.; Venkateswaran, G.; Shankar, J.; Gao, G.; Laurent, E.M.N.; et al. The interactome of metabolic enzyme carbonic anhydrase IX reveals novel roles in tumor cell migration and invadopodia/MMP14-mediated invasion. *Oncogene* **2017**, *36*, 6244–6261.
19. Lock, F.E.; McDonald, P.C.; Lou, Y.; Serrano, I.; Chafe, S.C.; Ostlund, C.; Aparicio, S.; Winum, J.-Y.; Supuran, C.T.; Dedhar, S. Targeting carbonic anhydrase IX depletes breast cancer stem cells within the hypoxic niche. *Oncogene* **2013**, *32*, 5210–5219.
20. Andreucci, E.; Ruzzolini, J.; Peppicelli, S.; Bianchini, F.; Laurenzana, A.; Carta, F.; Supuran, C.T.; Calorini, L. The carbonic anhydrase IX inhibitor SLC-0111 sensitises cancer cells to conventional chemotherapy. *J. Enzyme Inhib. Med. Chem.* **2019**, *34*, 117–123.

21. Boyd, N.H.; Walker, K.; Fried, J.; Hackney, J.R.; McDonald, P.C.; Benavides, G.A.; Spina, R.; Audia, A.; Scott, S.E.; Libby, C.J.; et al. Addition of carbonic anhydrase 9 inhibitor SLC-0111 to temozolomide treatment delays glioblastoma growth in vivo. *JCI Insight.* **2017**, *2*, e92928.
22. Alterio, V.; Cadoni, R.; Esposito, D.; Vullo, D.; Di Fiore, A.; Monti, S.M.; Caporale, A.; Ruvo, M.; Sechi, M.; Dumy, P.; et al. Benzoxaborole as a new chemotype for carbonic anhydrase inhibition. *Chem. Commun. (Cambridge)* **2016**, *52*, 11983–11986.
23. Nocentini, A.; Supuran, C.T. Carbonic anhydrase inhibitors as antitumor/antimetastatic agents: A patent review (2008–2018). *Expert Opin. Ther. Pat.* **2018**, *28*, 729–740.
24. Chia, S.K.; Wykoff, C.C.; Watson, P.H.; Han, C.; Leek, R.D.; Pastorek, J.; Gatter, K.C.; Ratcliffe, P.; Harris, A.L. Prognostic significance of a novel hypoxia-regulated marker, carbonic anhydrase IX, in invasive breast carcinoma. *J. Clin. Oncol.* **2001**, *19*, 3660–3668.
25. Tan, E.Y.; Yan, M.; Campo, L.; Han, C.; Takano, E.; Turley, H.; Candiloro, I.; Pezzella, F.; Gatter, K.C.; Millar, E.K.A.; et al. The key hypoxia regulated gene CA IX is upregulated in basal-like breast tumours and is associated with resistance to chemotherapy. *Br. J. Cancer* **2009**, *100*, 405–411.
26. Jing, X.; Yang, F.; Shao, C.; Wei, K.; Xie, M.; Shen, H.; Shu, Y. Role of hypoxia in cancer therapy by regulating the tumor microenvironment. *Mol. Cancer* **2019**, *18*, 157.
27. Svastová, E.; Zilka, N.; Zat'ovicová, M.; Gibadulinová, A.; Ciampor, F.; Pastorek, J.; Pastoreková, S. Carbonic anhydrase IX reduces E-cadherin-mediated adhesion of MDCK cells via interaction with β-catenin. *Exp. Cell Res.* **2003**, *290*, 332–345.
28. Liang, W.; Song, S.; Xu, Y.; Li, H.; Liu, H. Knockdown of ZEB1 suppressed the formation of vasculogenic mimicry and epithelial-mesenchymal transition in the human breast cancer cell line MDA-MB-231. *Mol. Med. Rep.* **2018**, *17*, 6711–6716.
29. Ferrari-Amorotti, G.; Chiodoni, C.; Shen, F.; Cattelani, S.; Soliera, A.R.; Manzotti, G.; Grisendi, G.; Dominici, M.; Rivasi, F.; Colombo, M.P.; et al. Suppression of invasion and metastasis of triple-negative breast cancer lines by pharmacological or genetic inhibition of slug activity. *Neoplasia* **2014**, *16*, 1047–1058.
30. Garrido-Castro, A.C.; Lin, N.U.; Polyak, K. Insights into molecular classifications of triple-negative breast cancer: Improving patient selection for treatment. *Cancer Discov.* **2019**, *9*, 176–198.
31. Salvatore, B.; Caprio, M.G.; Hill, B.S.; Sarnella, A.; Roviello, G.N.; Zannetti, A. Recent advances in nuclear imaging of receptor expression to guide targeted therapies in breast cancer. *Cancers (Basel)* **2019**, *11*, 1614.
32. Camorani, S.; Crescenzi, E.; Gramanzini, M.; Fedele, M.; Zannetti, A.; Cerchia, L. Aptamer-mediated impairment of EGFR-integrin αvβ3 complex inhibits vasculogenic mimicry and growth of triple-negative breast cancers. *Sci. Rep.* **2017**, *7*, 46659.
33. Hill, B.S.; Sarnella, A.; Capasso, D.; Comegna, D.; Del Gatto, A.; Gramanzini, M.; Albanese, S.; Saviano, M.; Zaccaro, L.; Zannetti, A. Therapeutic potential of a novel α v β_3 antagonist to hamper the aggressiveness of mesenchymal triple negative breast cancer sub-type. *Cancers (Basel)* **2019**, *11*, 139.
34. Ye, L.Y.; Chen, W.; Bai, X.L.; Xu, X.Y.; Zhang, Q.; Xia, X.F.; Sun, X.; Li, G.G.; Hu, Q.D.; Fu, Q.H.; et al. Hypoxia-induced epithelial-to-mesenchymal transition in hepatocellular carcinoma induces an immunosuppressive tumor microenvironment to promote metastasis. *Cancer Res.* **2016**, *76*, 818–830.
35. Wang, H.F.; Wang, S.S.; Zheng, M.; Dai, L.L.; Wang, K.; Gao, X.L.; Cao, M.X.; Yu, X.H.; Pang, X.; Zhang, M.; et al. Hypoxia promotes vasculogenic mimicry formation by vascular endothelial growth factor A mediating epithelial-mesenchymal transition in salivary adenoid cystic carcinoma. *Cell Prolif.* **2019**, *52*, e12600.
36. Wen, L.; Zong, S.Q.; Shi, Q.; Li, H.; Xu, J.; Hou, F. Hypoxia-induced vasculogenic mimicry formation in human colorectal cancer cells: Involvement of HIF-1a, Claudin-4, and E-cadherin and Vimentin. *Sci. Rep.* **2016**, *6*, 37534.
37. Pastorekova, S.; Gillies, R.J. The role of carbonic anhydrase IX in cancer development: Links to hypoxia, acidosis, and beyond. *Cancer Metastasis Rev.* **2019**, *38*, 65–77.
38. Ciccone, V.; Filippelli, A.; Angeli, A.; Supuran, C.T.; Morbidelli, L. Pharmacological inhibition of CA-IX impairs tumor cell proliferation, migration and invasiveness. *Int. J. Mol. Sci.* **2020**, *21*, 2983.
39. Guerrini, G.; Durivault, J.; Filippi, I.; Criscuoli, M.; Monaci, S.; Pouyssegur, J.; Naldini, A.; Carraro, F.; Parks, S.K. Carbonic anhydrase XII expression is linked to suppression of Sonic hedgehog ligand expression in triple negative breast cancer cells. *Biochem. Biophys. Res. Commun.* **2019**, *516*, 408–413.
40. Najafi, M.; Farhood, B.; Mortezaee, K.; Kharazinejad, E.; Majidpoor, J.; Ahadi, R. Hypoxia in solid tumors: A key promoter of cancer stem cell (CSC) resistance. *J. Cancer Res. Clin. Oncol.* **2020**, *146*, 19–31.

41. Gao, T.; Li, J.Z.; Lu, Y.; Zhang, C.Y.; Li, Q.; Mao, J.; Li, L.H. The mechanism between epithelial mesenchymal transition in breast cancer and hypoxia microenvironment. *Biomed. Pharmacother.* **2016**, *80*, 393–405.
42. Tong, W.W.; Tong, G.H.; Liu, Y. Cancer stem cells and hypoxia-inducible factors (Review). *Int. J. Oncol.* **2018**, *53*, 469–476.
43. Camorani, S.; Hill, B.S.; Collina, F.; Gargiulo, S.; Napolitano, M.; Cantile, M.; Di Bonito, M.; Botti, G.; Fedele, M.; Zannetti, A.; et al. Targeted imaging and inhibition of triple-negative breast cancer metastases by a PDGFRβ aptamer. *Theranostics* **2018**, *8*, 5178–5199.
44. Camorani, S.; Hill, B.S.; Fontanella, R.; Greco, A.; Gramanzini, M.; Auletta, L.; Gargiulo, S.; Albanese, S.; Lucarelli, E.; Cerchia, L.; et al. Inhibition of bone marrow-derived mesenchymal stem cells homing towards triple-negative breast cancer microenvironment using an anti-PDGFRβ aptamer. *Theranostics* **2017**, *7*, 3595–3607.
45. Zannetti, A.; Iommelli, F.; Fonti, R.; Papaccioli, A.; Sommella, J.; Lettieri, A.; Pirozzi, G.; Bianco, R.; Tortora, G.; Salvatore, M.; et al. Gefitinib induction of in vivo detectable signals by Bcl-2/Bcl-xL modulation of inositol trisphosphate receptor type 3. *Clin. Cancer Res.* **2008**, *14*, 5209–5219.
46. Zannetti, A.; Del Vecchio, S.; Romanelli, A.; Scala, S.; Saviano, M.; Cali', G.; Stoppelli, M.P.; Pedone, C.; Salvatore, M. Inhibition of Sp1 activity by a decoy PNA-DNA chimera prevents urokinase receptor expression and migration of breast cancer cells. *Biochem. Pharmacol.* **2005**, *70*, 1277–1287.
47. Pelagalli, A.; Nardelli, A.; Fontanella, R.; Zannetti, A. Inhibition of AQP1 hampers osteosarcoma and hepatocellular carcinoma progression mediated by bone marrow-derived mesenchymal stem cells. *Int. J. Mol. Sci.* **2016**, *17*, 1102.
48. Fontanella, R.; Pelagalli, A.; Nardelli, A.; D'Alterio, C.; Ieranò, C.; Cerchia, L.; Lucarelli, E.; Scala, S.; Zannetti, A. A novel antagonist of CXCR4 prevents bone marrow-derived mesenchymal stem cell-mediated osteosarcoma and hepatocellular carcinoma cell migration and invasion. *Cancer Lett.* **2016**, *370*, 100–107.
49. Zannetti, A.; Iommelli, F.; Speranza, A.; Salvatore, M.; Del Vecchio, S. 3′-deoxy-3′-18F-fluorothymidine PET/CT to guide therapy with epidermal growth factor receptor antagonists and Bcl-xL inhibitors in non-small cell lung cancer. *J. Nucl. Med.* **2012**, *53*, 443–450.
50. Aloj, L.; Zannetti, A.; Caracó, C.; Del Vecchio, S.; Salvatore, M. Bcl-2 overexpression prevents 99mTc-MIBI uptake in breast cancer cell lines. *Eur. J. Nucl. Med. Mol. Imaging* **2004**, *31*, 521–527.